European Wind Energy Conference and Exhibition
2010, Warsaw, Poland

ewec 2010 WARSAW
Europe's premier wind energy event
Warsaw, Poland, 20-23 April 2010

Preliminary results of a statistical wind resources analysis in offshore conditions in the Eastern Gulf of Mexico

PO.89

Rolando Soler-Bientz[1,2*], Simon Watson[1], David Infield[3]
[1] CREST, Electronic and Electrical Engineering, Loughborough University, UK
[2] Energy Laboratory, Faculty of Engineering, Autonomous University of Yucatan, México. *email: sbientz@msn.com
[3] Institute of Energy and Environment, University of Strathclyde, UK

ABSTRACT

A statistical analysis of the wind resources has been undertaken by mean of data measured on a communication tower installed on a pier which extends 6.65km from the coastline. A set of wind and temperature sensors were installed to record the ten minute averages over approximately two years. As a complement, hourly values of Sea Surface Temperature, extracted from GEOS satellite measurements over the study region, were also included in the research presented. The results have confirmed that the offshore wind is thermally driven by differential heating of land and sea producing sea breezes which veer to blow parallel to the coast in the late afternoon under the action of the Coriolis force. Air temperature and sea surface temperature profiles suggested largely unstable conditions and the potentially development of a shallow Stable Internal Boundary Layer.

1. INTRODUCTION

In offshore conditions, the differences between the air and sea temperatures, water depth and distance from the coastline are among the principal factors influencing the wind speeds and the stability conditions in the atmospheric boundary layer. The flow of winds over a coastal discontinuity face changes in roughness, availability of heat and moisture which alter the turbulent mixing and momentum transfer creating different stability conditions in offshore sites and influencing the wind profile behaviour [1]. By means of data measured from an offshore wind farm in Denmark, Barthelmie studied the changes in the onshore and offshore stability and their impact in the wind profile [2].

In the case of offshore conditions, Van Wijk et al. [3] obtained good estimates for the seasonal mean wind speed in the North Sea after applying their "diabatic" method to calculate the wind speed profile as a function of height, when wind speed, sea water temperature and air temperature are known. This diabatic method was also used by Coelingh et al. to study offshore [4] and onshore sites [5]. These two studies of the North Sea and its coastal areas concluded that diurnal variations are very similar in autumn and winter and that the thermal circulation leads to sea breezes with important effects up to 30km offshore for wind speeds lower than 7m/s.

For the marine environment of the Danish Baltic Sea, Lange et al. [6] studied the influence of thermal effects on wind speed profiles reporting that the standard Monin-Obukhov theory predicted lower wind speed values than measured for stable and near-neutral conditions, especially at large distances from the shore. Using wind speed and air temperature data measured from one onshore site and two offshore towers, Pryor and Barthelmie [7] studied the wind speed, stability and surface roughness. They reported that wind speed distributions onshore and offshore were statistically different for heights less than 20m regardless of the atmosphere stability conditions, at distances less than 2km from the shore. In an extended study using data from the Danish monitoring network [8], the same authors concluded that sites located within 2km from the coastline could experience significant vertical shear and differing turbulence because the wind speeds close to the sea surface were frequently decoupled from the wind characteristics above 30m in height.

Lapworth [9] reported diurnal patterns with maximum winds overnight and minimum values occurring during the afternoon for the offshore surface winds around the English coast after applying numerical models for stable boundary layers to offshore measurements made in static vessels. On the other hand, Barthelmie et al. [10] studying the coastal meteorology of Denmark found that the offshore sites which receive winds from over the land showed a typical onshore pattern with lowest wind speeds overnight and highest wind speeds during the afternoon. Generally, the increase in offshore wind speeds overnight is produced by the lower roughness of the sea surface and the transition from stable conditions over land to less stable conditions over sea. During the day, the transition from unstable conditions over land to stable conditions offshore means that the surface layer becomes decoupled from higher wind speeds aloft and the wind speed close to the surface layer is lower, as was reported by Barthelmie at al. [11].

In the case of the Yucatán Peninsula; the temporal, spatial and vertical wind characteristics have been already studied for sites located inland and onshore of this region [12, 13, 14]. Also, a preliminary analysis undertook in the North-East coast of the Yucatán Peninsula [15] revealed unexpected high wind shear not well represented by the Monin-Obukhov similarity theory. Therefore, in order to understand the sources of so high values of wind shear, this paper has been focused in the analysis of data recorded over two years at 6.65km offshore of the North coast of the Yucatán Peninsula. The measurements were recorded using a 25m height communication tower installed at the end of a long pier that runs almost perpendicular to the shoreline.

2. ONSITE MEASUREMENTS

The site that was available for the offshore study in this research is located at the end of the "Progreso" pier. This pier extends 6.65km into the Gulf of México from the North shore of the Yucatán Peninsula with geographical coordinates: 21°20'45.18"N, 89°40'17.32'W. The mast erected on this pier that was available to this study will be referred to as the API tower. Figure 1 below shows satellite images of the pier and the location of the measurement tower close to the end of the pier on its east side.

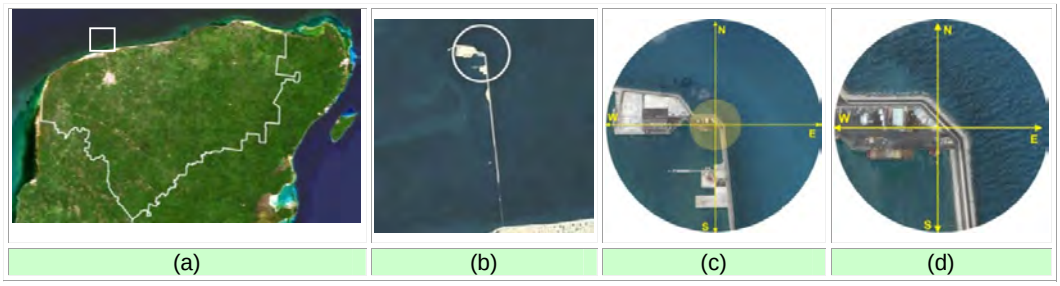

Figure 1. (a) Location of the "Progreso" pier in relation to the Yucatán Peninsula, (b) location relative to the North shore, (c) One kilometre radius and (d) 250m radius around measurement tower.

The terrestrial view of the API tower in Figure 2 shows a solid cylinder, located above the pier surface, of 1m diameter at the tower base and 70cm at the top of the tower. The relative position of the sensors, wind and air temperature, are also shown in the same Figure. These sensors were installed on a boom at a distance of at least 1.5m from the side of the tower, at 10m and 25m height over the pier surface.

Figure 2. Different terrestrial views of the measurement tower showing the location of the tower on the pier and the position of the sensors on the tower.

The measurements were taken continuously during 23 months starting in August 2007. A total of 87470 records of 10-minute averaged values were available after filtering for measurement errors. Figure 3 shows the data available for each month over the whole measurement period. As can be seen, less than the 50% of

the data were available during May and June due to maintenance problems at the end of the first year of measurement.

Figure 3. Data availability by month over the whole measurement period.

3. WIND PATTERNS

3.1 Directional distribution of the measurements

The distribution of the direction data using 22.5 degree bins to cover 16 directional sectors is shown in Figure 4. The symbol "lo" will represent the 10m height and "hi' will represent 25m height in the next figures unless any other meaning is specified.

Figure 4(a) shows that the winds at both measurement heights are mainly distributed in a region from the N to the SSE sectors, in a clockwise direction. The majority of the sectors outside of this region receive just less than 1% of the winds available. The wind direction distribution is clustered around a principal maximum in the NE-ENE sectors and around a secondary maximum in the ESE-SE sectors.

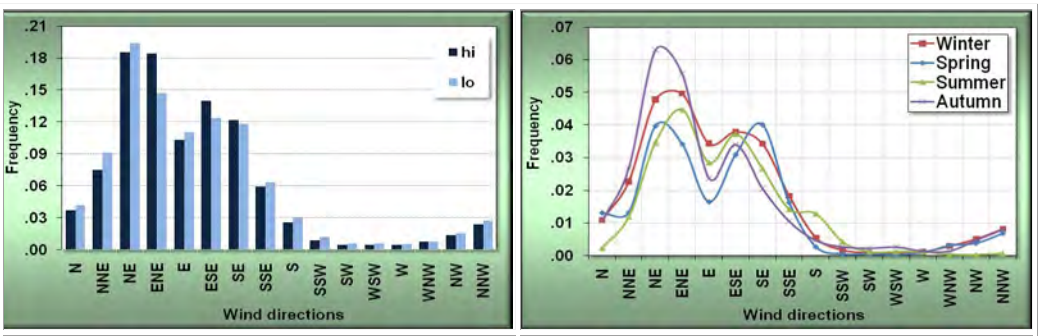

Figure 4. Frequency distribution by direction of the measurements over the whole study period: (a) at both measurement heights and (b) during every season for the "hi" height measurements.

In Figure 4(b), the months were grouped by season: Winter (December, January and February), Spring (March, April and May), Summer (June, July and August) and Autumn (September, October and November), the distribution of wind direction for each season at the "hi" height shows that all seasons displayed broadly the same distribution shown in Figure 4(a) but there is some variation in the fraction of measurements in the NE-ENE sectors, with the greatest number seen during the Autumn season.

Figure 5 shows, every three hours during the day, the frequency distributions of the data measured for each directional sector over the whole study period. The time period when the atmosphere goes from cooling to heating is shown in Figure 5(a) from midnight up to 9:00 in the middle of the morning. The transition between heating and cooling, from midday to 21:00 hours, can be seen in Figure 5(b).

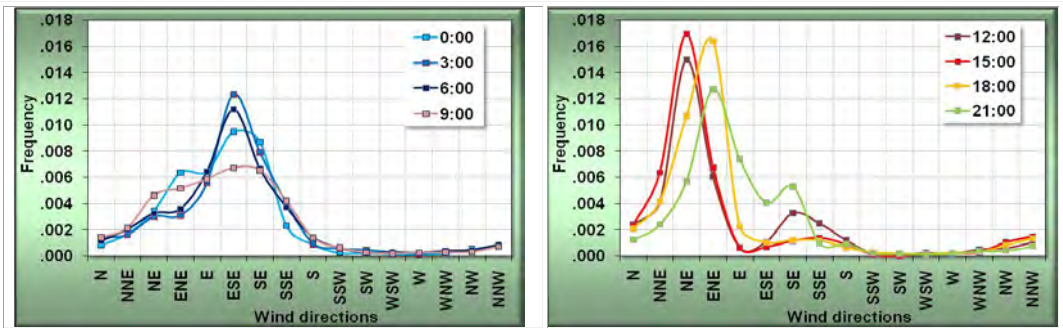

Figure 5 Directional frequency distributions for the data measured at 8 different hours over the whole study period: (a) from midnight up to before midday, (b) from midday up to before midnight.

3.2 Diurnal distribution of the main winds

Figure 6 shows the frequency distributions of the main 8 directional sectors, from N to SSE during the diurnal cycle, using the measurements recorded over the whole study period. The distributions for directional sectors between E and SSE shown in Figure 6(a) represent the contribution of the winds coming from the land located at the North East of the Yucatán Peninsula, see Figure 1(a). The winds coming from the sea located around the North East of the Gulf of México are represented by the directional sectors from N to ENE, see Figure 6(b).

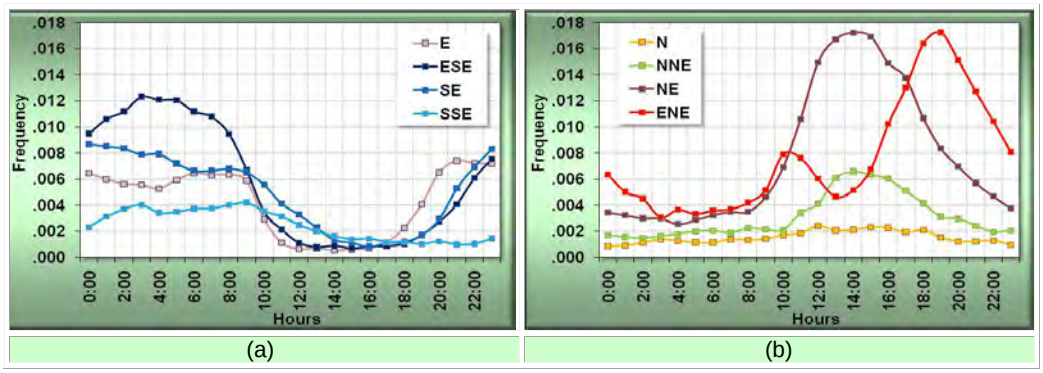

Figure 6 Diurnal frequency distributions for the main directional sectors over the whole study period: (a) for winds coming from the land, (b) for winds coming from the sea.

Figure 5(a) and Figure 6(a) indicate that in the morning the wind is coming predominantly off the land, but this starts to back towards the NE between sunrise and noon. Figure 5(b) and Figure 6(b) show that between 12:00 and 15:00 the wind is coming predominantly from the sea. Later in the afternoon and evening the wind veers somewhat so that it is more parallel to the coast. This would seem indicative of a thermally driven sea breeze developing off the North coast of the Yucatán Peninsula which changes direction during the late afternoon as the Coriolis force takes effect.

3.3 Wind speed averages

The aggregated 10 minute wind speed averages are shown in Figure 7 (a), (b) and (c) as a function of direction, time of day and month of the year, respectively. The highest wind speeds are seen to come from the ENE direction which also shows the greatest difference between the “hi” and “lo” wind speed averages with approximately 2m/s faster average wind speed at “hi” height. This winds coming off the sea tend to be greater in magnitude than those off the land which probably reflects the lower surface roughness.

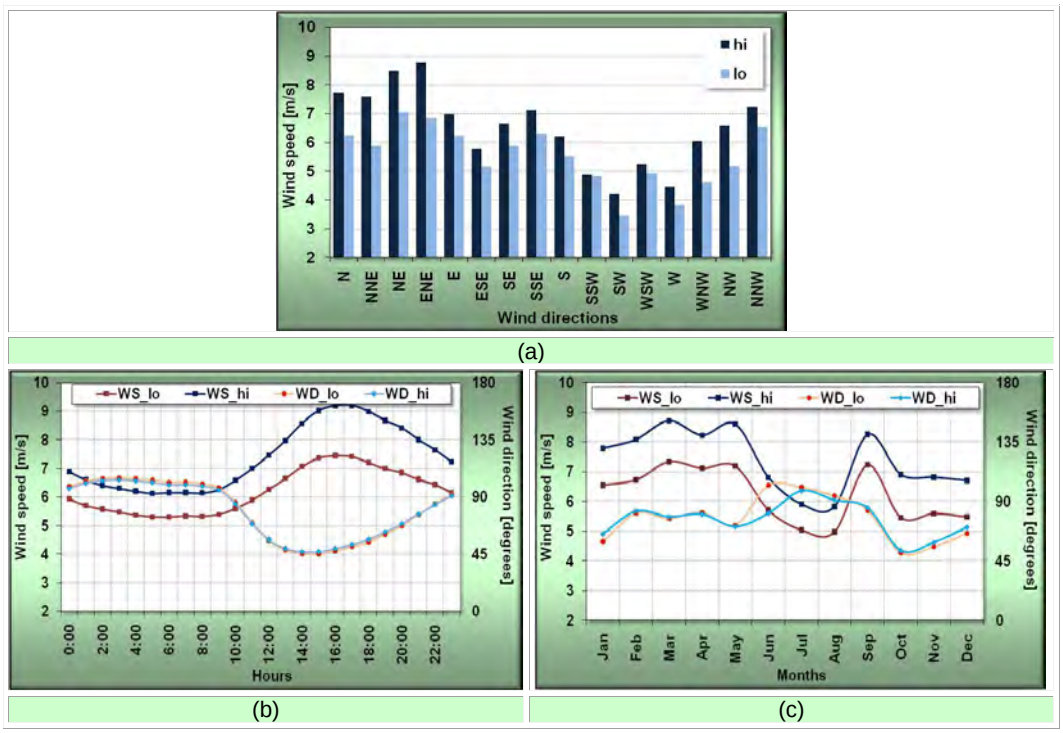

Figure 7. Wind speed averages over the whole study period for each direction (a), diurnal cycle (b) and seasonal pattern (c).

Figure 7(b) shows that there is a relatively constant wind speed and wind direction from midnight to early morning when the winds are mainly coming from the land around the 90 degree direction, see Figure 1(a) and (b). From early morning to 14:00 in the afternoon, the winds gradually increase their intensity changing their direction to North East. At 16:00, the maximum speed is reached and the difference between the "hi" and "lo" wind also reaches its maximum. The wind direction then returns to 90 degrees from 16:00 to midnight while the wind speed decreases gradually over this period. The behaviour seen at these sites represents the combination of thermally driven winds, the effect of the sea-breeze and the effect of surface roughness, where the winds coming over the smoother sea fetch tend to be higher.

Figure 7(c), shows a decrease in the wind speed in June, July and August; followed by a peak during September and a relatively constant wind speed during the rest of the year. The mean wind direction shows that the highest wind speeds are observed when the wind is coming from the ENE-E and reduce when the winds come from the ESE. This behaviour is again consistent with conditions described in the previous paragraph when analysing the diurnal behaviour.

4. TEMPERATURE ANALYSIS

4.1 Onsite air temperature

Figure 8 shows the average air temperature as a function of time of day and season at both measurement heights over the whole study period. The diurnal pattern in Figure 8(a) shows a maximum around 12:00 which decreases steadily reaching a minimum at 06:00. A difference of approximately 2^{o}C between the temperature at "lo" and "hi" height is present during the day which on this initial evidence would suggest a very unstable convective boundary layer.

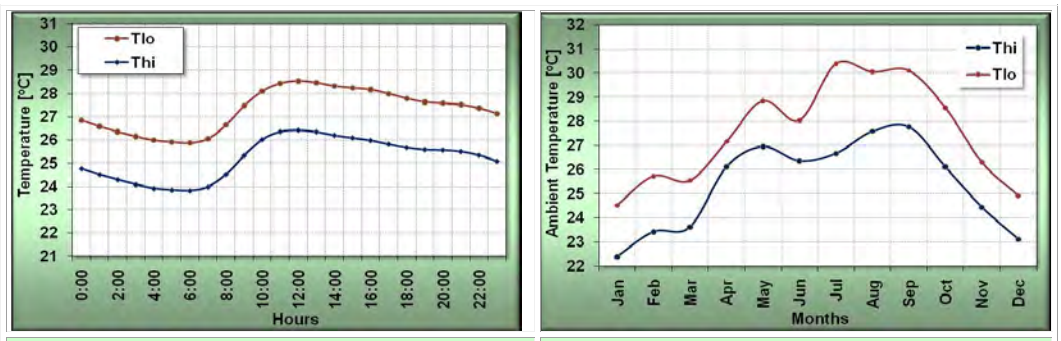

Figure 8. Average of ambient temperature at both measurement heights: (a) Diurnal pattern and (b) Seasonal pattern

The seasonal pattern in Figure 8(b) displays the double peak already described in previous research [14] which is related to the rainy season in June-July.

4.2 Satellite thermal images

The NOAA's GOES (Geostationary Operational Environmental Satellites) are located in geo-stationary orbit above the Western Hemisphere. This characteristic enables measurements of one hour gridded sea surface temperatures aligned by longitudes from 179.975 W to 30.025 W and by latitudes from 59.975 N to 44.975 S with a spatial resolution of 0.05 degrees. The GOES SST data was obtained from the JPL Physical Oceanography DAAC (Distributed Active Archive Center) [16]. Using a decoding algorithm from NOAA, an application was developed to extract SST data expressed in degree Celsius from binary data format satellite maps.

Figure 9(a) and (b) show the geographical areas of the Gulf of México and the selected region around the "Progreso" Pier respectively. Their extracted SST images are shown in Figure 9(c) and (d).

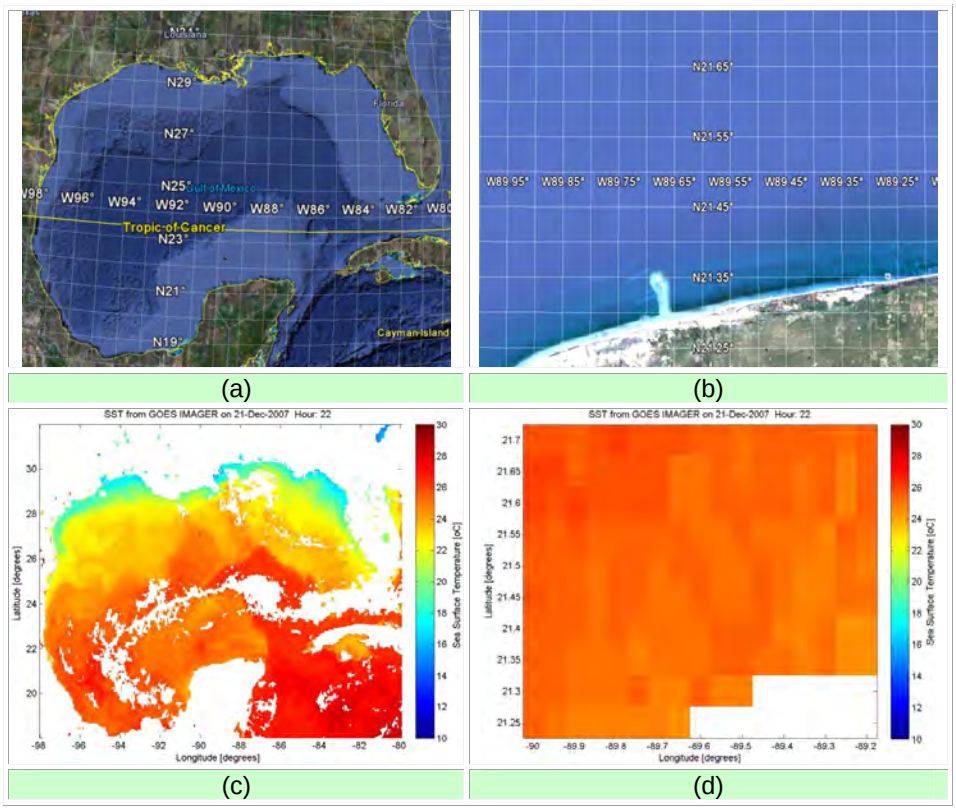

Figure 9. (a) Gulf of México and (b) "Progreso" pier areas with an example of an SST temperature map for each region (c) and (d).

4.3 Satellite SST data for the study period

A time period between 25/07/2007 and 26/06/2009 was selected covering the period of measurements recorded on the API mast (703 days). A total of 38.5% SST values concurrent with the mast measurements was successfully extracted from the GEOS satellite thermal images corresponding to 6500 hourly values. Figure 10 below shows the distribution of SST data available binned by hour of the day and averaged over the entire study period.

Figure 10. SST data available from GEOS Satellite during the day averaged over the entire study period between 25/07/2007 and 26/06/2009.

Figure 11(a) below show the daily averages of the satellite SST data over the whole study period. The peaks in the seasonal temperature pattern discussed in previous papers [14], are identifiable in September 2008 and May 2009 as well as the minimum between December and January of each year.

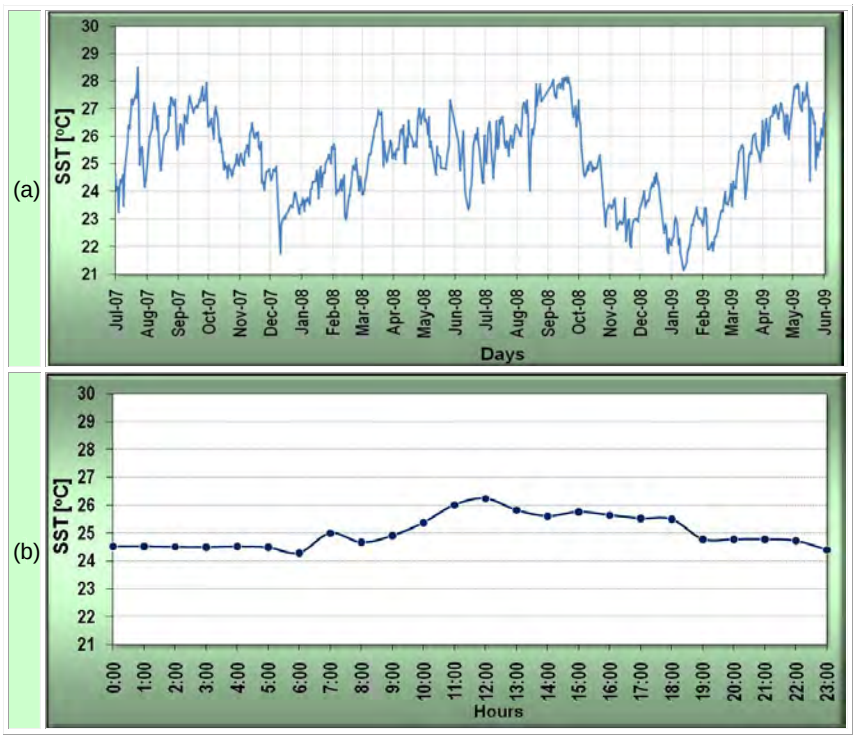

Figure 11. Averages of SST from the GEOS Satellite over the whole study period: (a) daily and (b) hourly.

Hourly averages of the Satellite SST over the whole study period were computed and are shown in Figure 11(b). Though the SST varies little during the day, on average there is evidence of a diurnal cycle.

4.5 Vertical temperature profile

Averages of the measured temperature as a function of height have been plotted in Figure 12, for the whole study period, for every three hours during the day. The temperature trends over the day at all heights display a diurnal cycle with the highest temperature at noon and the lowest just around sunrise, e.g. 06:00. However, the ranges of temperatures differ: there is range of around 6 degrees Celsius at 10m and 25m height, but the range at the sea surface is less than 2 degrees Celsius. This is as one would expect due to the high thermal mass of the water. What is interesting to note is the lapse rate between 0m and 10m and that between 10m and 25m height. The temperatures at 10m and 25m would suggest very unstable conditions throughout the day, whereas those between 0m and 10m would suggest stable or close to neutral conditions with the most stable conditions at midday and the least stable (closer to neutral) at sunrise (06:00).

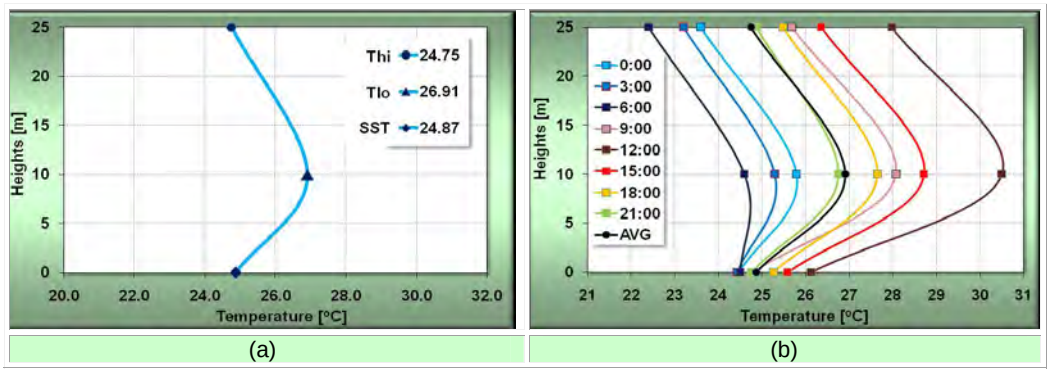

Figure 12. Vertical temperature profile using the measurements from the GEOS Satellite for SST and from the API mast at "hi" and "lo" heights: (a) average over the whole study period (b) hourly averages for selected times of the day.

For conditions where the wind blows off warmer land onto colder sea, a stable thermal internal boundary layer SIBL grows offshore as a result of the advection, driven by the geostrophic wind. This is due to the wind flow offshore of well mixed air from the land resulting from convective turbulence created by the heating of the land from sunrise until the early afternoon [17].

The results presented above, would suggest that initially, after sunrise, the wind blows off the land over the sea. This results in a layer of warm air advecting over the sea and the development of a thin Stable Internal Boundary Layer (SIBL) [19] which growth rate as function of the distance to the coast is less than 10^{-3} [20, 21]. As the day develops, a more onshore sea breeze results which eventually veers to be parallel to the coast and after sunset reverts to a more offshore breeze with cooler air advecting over the sea and a diminishing of the SIBL with the development of a more Convective Boundary Layer (CBL) at night until the cycle is repeated the following day [22, 18]. This is an example of an inverted diurnal cycle (compared to the land).

5. CONCLUSIONS

The wind speed and direction measured in the offshore conditions of the API site follow the expected pattern of a diurnal cycle produced by the difference in the heating rates between the land and the sea which drive alternating pressure gradients. There is also a significant influence of the Coriolis force which causes the sea breeze to blow in a direction more parallel to the shoreline of the North of the Yucatán Peninsula later in the afternoon.

The analysis of the offshore data revealed a non-uniform surface boundary layer and it is clear that more detailed profile measurements are required offshore to gain greater insight into the atmospheric boundary layer offshore. The application of numerical models, e.g. mesoscale models, would help to give more detail on the horizontal and vertical fluxes in this region.

REFERENCES

1. Kaimal JC, Finnigan JJ. Atmospheric Boundary Layer Flows: Their Structure and Measurement. Oxford University Press, New York, 1994.

2. Barthelmie RJ. The effects of atmospheric stability on coastal wind climates. Meteorol. Appl. 1999; 6:39-47.
3. Van Wijk AJM, ACM Beljaars, AAM Holtslag and WC Turkenburg. Evaluation of stability corrections in wind speed profiles over the North Sea, Journal of Wind Engineering and Industrial Aerodynamics 1990;33: 551–566.
4. Coelingh JP, AJM van Wijk and AAM Holtslag. Analysis of wind speed observations over the North Sea, Journal of Wind Engineering and Industrial Aerodynamics 1996;61(1): 51-69.
5. Coelingh JP, AJM van Wijk and AAM Holtslag. Analysis of wind speed observations on the North Sea coast, Journal of Wind Engineering and Industrial Aerodynamics 1998;73(2): 125-144.
6. Lange B, Larsen S, Højstrup J and Barthelmie RJ. The influence of thermal effects on the wind speed profile of the coastal marine boundary layer, Boundary Layer Meteorology 2004;112: 587–617.
7. Pryor SC and Barthelmie RJ. Analysis of the effect of the coastal discontinuity on near-surface flow, Annals of Geophysics 1998;16: 882–888.
8. Pryor SC and Barthelmie RJ. Statistical analysis of flow characteristics in the coastal zone, Journal of Wind Engineering and Industrial Aerodynamics 2002;90(3): 201-22.
9. Lapworth A. The diurnal variation of the marine surface wind in an offshore flow, Quarterly Journal of the Royal Meteorological Society 2005;131(610), Part B: 2367-2387.
10. Barthelmie RJ, Courtney MS, Højstrup J and Larsen SE. Meteorological aspects of offshore wind energy: observations from the Vindeby wind farm, Journal of Wind Engineering and Industrial Aerodynamics 1996;62: 191-221.
11. Barthelmie RJ, Grisogono B and Pryor SC. Observations and simulations of diurnal cycles of near-surface wind speeds over land and sea, Journal of Geophysical Research, 1996;101(D16): 21327–21337.
12. Soler-Bientz R, Watson S and Infield D. Preliminary study of long-term wind characteristics of the Mexican Yucatán Peninsula. Energy Conversion and Management, 2009. 50(7): 1773-1780.
13. Soler-Bientz R, Watson S and Infield D. Evaluation of the Wind Shear at a Site in the NorthWest of the Yucatan Peninsula, Mexico. Wind Engineering, 2009. 33(1): p. 93-107.
14. Soler-Bientz R, Watson S and Infield D. Wind characteristics on the Yucatán peninsula based on short term data from meteorological stations. Energy Conversion and Management, 2010. 51(4): 754-764.
15. Soler-Bientz R, Watson S and Infield D, Study of the offshore wind and its propagation inland of the northern zone of the Yucatan Peninsula, Eastern Mexico, EWEC2009, Marseille, France, March 2009.
16. JPL Physical Oceanography DAAC (Distributed Active Archive Center). GOES SST data. Web site (ftp://podaac.jpl.nasa.gov/pub/sea_surface_temperature/goes/goes11-12/data/), 2009, [retrieved [01.07.09].
17. Mulhearn PJ. On the Formation of a Stably Stratified Internal Boundary Layer by Advection of Warm Air over a Cooler Sea, Boundary Layer Meteorology 1981;21: 247-254.
18. Kaimal JC and Finnigan JJ. Atmospheric Boundary Layer Flows: Their Structure and Measurement. Oxford University Press, New York, 1994.
19. Stull RB, An Introduction to Boundary Layer Meteorology, Kluwer Academic Publishers, Dordrccht, The Netherlands, 1988.
20. Garratt JR. The Stably Stratified Internal Boundary Layer for Steady and Diurnally Varying Offshore Flow, Boundary Layer Meteorology, 1987;38: 369-394.
21. Garratt, J.R. and Ryan B.F. *The structure of the stably stratified internal boundary layer in offshore flow over the sea.* Boundary Layer Meteorology 1989;**47**(1): 17-40
22. Hsu SA. On the Growth of a Thermally Modified Boundary Layer by Advection of Warm Air Over a Cooler Sea, Journal of Geophysics Research 1983;88: 771-774.